Cryogenic cooling and cutting system: A novel cutting technique for offshore monopile foundations

Kenneth Bisgaard Christensen[a], **Shahin Jalili**[b], **Alireza Maheri**[a,*]

[a]*School of Engineering, University of Aberdeen, King's College, Aberdeen AB24 3UE, United Kingdom*
[b]*National Decommissioning Centre, University of Aberdeen, Newburgh, Ellon AB41 6AA, United Kingdom*

Abstract:

This paper presents a feasibility study of a new embrittlement-cutting technique for offshore wind monopile foundations called Cryogenic Cooling and Cutting System (CCCS). The main idea of CCCS is based on the cryogenic treatment of monopile wall surface to reduce its impact energy absorption capability and achieve faster-cutting speeds in comparison to conventional cutting techniques. The overall idea and proof of concept of the CCCS are presented and the cutting process using the CCCS is simulated using a finite difference-based heat transfer model. The overall performance of CCCS is assessed in comparison to the conventional AWJ technique in terms of cutting speeds and times. The sensitivity of the CSSS technique to different parameters, such as ambient temperature, cooling bandwidth, and monopile length, are also investigated. The numerical results from the heat transfer analysis and real-world offshore wind decommissioning project suggest that the new CCCS cutting technique can offer faster-cutting speeds with the potential capability of reducing offshore wind farm decommissioning costs.

Keywords: Cryogenic cooling and cutting system, embrittlement cutting, offshore wind farm, decommissioning, foundations

Abbreviations:

Abrasive Water Jet	AWJ	Meteorological Mast	MM
American Society of Mechanical Engineering	ASME	Offshore Substation	OS
Barge Vessel	BV	Offshore Support Vessel	OSV
Cryogenic Cooling and Cutting System	CCCS	Offshore Wind Farm	OWF
Dimond Wire	DW	Oil and Gas	O&G
Ductile to Brittle Transition Temperature	DBTT	Oxy Arc Cutter	OAC
Finite Difference Method	FDM	Plasma Arc	PA
International Organisation for Standardisation	IOS	Remotely Operated Vessel	ROV
Jack-Up Vessel	JUV	Shear Ram	SR
Laser Beam	LB	Tug Boat	TB
Liquid Nitrogen	LN_2	Wind Turbine	WT

1. Introduction

The global climate emergency has intensified the efforts to create clean, renewable energy resources worldwide to reduce greenhouse gas emissions and keep the average global temperature under control. Offshore wind is one of the key renewable energy resources that has witnessed a considerable expansion during the past two decades [1]. The European Union and

*Corresponding author, email: alireza.maheri@abdn.ac.uk

the UK are global leaders in offshore wind energy, with total capacities of 14.60 GW and 10.40 GW, respectively, reported in 2020 [2]. The success of previous Offshore Wind Farm (OWF) projects and the urgent need for clean energy have convinced policymakers to further support and boost the global offshore wind energy capacity in the coming decades. For example, the UK government has recently set a plan to expand the offshore wind capacity to 40 GW by 2030, which is in line with the country's policy to meet the net zero emission target by 2050 [3]. The European Union has also implemented an ambitious plan to install a large number of WFs in the coming decades and boost their overall wind energy capacity to 450 GW by 2050 [4], [5].

In addition to the rapid expansion, the offshore wind sector has also achieved remarkable development from the technological aspects of OWF assets, resulting in shorter installation times and cheaper energy production costs [6]. However, the limited operational lifetime of OWFs is still a big challenge. The performance of previously erected OWFs suggests that their operational lifetime is typically between 20 and 25 years [7]–[9]. This highlights the fact that a huge number of OWFs will be required to be decommissioned in the near future, which can create another environmental challenge [10]. The decommissioning process includes a set of actions that need to be performed to return the OWF site to its original state before the installation. The Wind Turbines (WTs), Offshore Substation (OS), Meteorological Mast (MM) and their foundation needs to be dismantled and removed from the seabed, while the cables and scour protection can be left in their situ based on current regulations if they do not put any risk for marine navigation. However, the current regulations in different countries on cables may change in the near future, and they may need to be fully removed from the seabed. The OWF decommissioning operations are typically performed by expensive vessels/equipment that needs to be properly managed under harsh and uncertain weather conditions.

One of the expensive OWF decommissioning activities is the WT foundation removal which requires subsea cutting and lifting operations. Most of the current OWFs approaching the decommissioning stage are in shallow waters with tubular monopile foundations [11]. In comparison to other foundation types, the monopile is a popular structural option for WT foundations due to its simple design, lower cost, ease of fabrication, and straightforward installation [12], [13]. According to Gupta and Basu [13], the foundations of almost 80% of current OWFs is steel tubular monopiles. The monopile foundation removal operation is usually performed by a Jack-Up Vessel (JUV) and Offshore Support Vessel (OSV) supported by the appropriate number of Barge Vessels (BVs) and Tug Boats (TBs) for transportation. A Remotely Operated Vessel (ROV) is also required to support the subsea cutting and excavation operations. The monopiles are usually cut from 1 m under the seabed by an appropriate cutting tool [14] and lifted by a JUV on a BV.

The historical development of OWFs shows that the sizes of monopile foundations have gradually increased during the past two decades as a result of an increase in WT unit capacities. The diameter of current monopile foundations varies between 4 m and 8 m [12]. With the current appetite for further expansion of wind energy capacity, the new generation of OWFs is expected to be installed in deeper waters with larger WT units which will require larger monopile foundations with up to 10 m in diameter [13], [15]. This makes the foundation removal operation

even more expensive as the larger monopile foundations will result in longer cutting and removal durations as well as higher decommissioning costs at the end of the operational lifetime of OWFs. The fast, efficient cutting techniques can potentially reduce the rental duration of expensive vessels/equipment employed at the decommissioning stage. Moreover, the currently available cutting techniques, such as the Abrasive Water Jet (AWJ) tool, are energy-intensive tools with certain environmental impacts [16], [17]. Hence, the development of faster, cheaper, and environment-friendly foundation-cutting techniques is crucial to reduce the economic and environmental impacts of OWF decommissioning projects.

Cryogenic is a heat treatment approach performed at unconventionally lower temperatures with the primary purpose of improving the mechanical properties of materials [18], [19]. The cryogenic treatment process is usually delivered through liquid gasses, such as Liquid Nitrogen (LN_2) [20]. The cryogenic treatment has been widely employed for the optimisation and improvement of mechanical properties of steel, such as fatigue and hardness [21]–[24]. For example, Li et al. [21] investigated the effects of deep cryogenic treatment on steel hardness, in which the steel is submerged in a bath of coolant (e.g., LN_2) for a given time to increase the hardness and reduced its grain size. The study confirmed that the tensile and fatigue strengths of steel could be improved by the deep cryogenic treatment. In another study, Sivaiah and Chakradhar [25] investigated the effects of cryogenic cooling on a set of performance characteristics in the machining process of 17-4 PH stainless steel. The study reported the effectiveness of cryogenic cooling in improving the performance characteristics of the machining process. In recent years, the cryogenic cooling process has also been employed to reduce the surface temperature of steel during the milling processes [26], [27].

Cryogenic cooling has also been applied to enhance the performance of cutting tools in different aspects, such as their wear resistance, tool life, dimensional integrity, and product quality [19]. The review provided by Akincioğlu et al. [19] reveals that the cryogenic treatment process can reduce cutting tool costs due to a prolonged lifespan and corrosion resistance. The cryogenic cooling treatment provides a fast-machining process, as it allows the cutting tool to operate at lower forces with higher cutting speeds [28].

The embrittlement cutting is a novel idea that aims to take advantage of Ductile to Brittle Transition (DBTT) behaviour in mild carbon steel types caused by their high iron (Fe) content with a body-centred cubic atomic structure. The mild carbon steels exhibit a highly impacted DBTT depending on temperature, which makes them brittle at lower temperatures and significantly decreases their impact energy absorption capability [29]. This study presents a feasibility investigation of a new embrittlement technique for cutting offshore wind monopile foundations, called Cryogenic Cooling and Cutting System (CCCS). The main idea of CCCS is based on the cryogenic treatment of the mild steel object to achieve lower impact energy required for the cutting process. The intention is to achieve a faster cutting process in comparison to conventional cutting techniques in the offshore wind industry. The study investigates the practical application of the proposed technique in cutting the monopile foundations in the OWFs. The performance of the proposed CCCS technique is compared to the traditional non-thermal cutting technique of AWJ based on a heat transfer analysis. The study also discusses how the

development of the new CCCS technique can reduce the duration and costs of OWF decommissioning projects.

The rest of the paper is organised as follows. Section 2 gives a brief overview of currently available cutting techniques in the offshore industry. The proof of concept and the heat transfer analysis model for the novel CCCS technique are discussed in Section 3. Section 4 investigates the performance of the CCCS technique in terms of cutting times and speeds based on the heat transfer analysis and provides the potential economic benefits of the CCCS for the OWF decommissioning projects. Finally, Section 5 provides the concluding remarks.

2. Overview of cutting techniques employed in the offshore industry

The currently employed cutting techniques in the offshore industry can be categorised into Dimond Wire (DW), AWJ, Laser Beam (LB), Plasma Arc (PA), Oxy Arc Cutter (OAC), explosives, and Shear Ram (SR) techniques. The mentioned cutting techniques have been widely employed for different cutting purposes in the Oil and Gas (O&G) industry. The applicability of each cutting technique depends on the foundation diameter and wall thickness. The PA and explosives techniques are not appropriate options for monopile cutting operations as their performance highly depends on the wall thickness. The applicability of the SR technique primarily depends on the monopile diameter rather than thickness, and their design is not flexible enough to handle large diameters of monopile foundations [30]. Moreover, there are safety concerns in the application of OAC, as it requires risky manual labour operation. The DW is a well-developed external cutting technique in which the excavation around the monopile is needed to provide access of cutting equipment to the cutting line.

The AWJ is the most popular cutting technique for monopile foundation removal in OWF decommissioning projects. The AWJ is an internal and automated cutting method applicable to monopiles with a wide range of diameters and thicknesses, which can reduce the costs and risk for the operators. Table 1 presents the comparison of the different conventional cutting techniques employed in the industry based on different performance measures, including type, cutting cost, speed, productivity, precision, quality, energy consumption, safety risks, environmental impact, ambient applicability, material applicability as well as the maximum thickness that they can cut. The table clearly shows the advantages and disadvantages of each cutting technique. As the AWJ is widely applied for monopile foundation cutting in OWF decommissioning projects, this study will assess the performance of the new cutting concept against the AWJ technique. The following subsection discusses the AWJ cutting technique in more detail.

Table 1. Comparison of the different conventional cutting techniques employed in the industry based on different performance measures [30]–[39]

	DW	AWJ	LB	PA	OA	SR	Explosives
Type	External	External/Internal	External/Internal	External/Internal	External/Internal	External	External/Internal
Cost	High	Highest	Medium	Low	Lowest	Medium	Low
Speed	Low	Low	High	Highest	Medium	High	Instant
Productivity	Medium/Low	Low	Highest	High	Low	High	Lowest
Precision	High	Highest	Medium	High	Low	Lowest	Lowest
Quality	High	Highest	Medium	low	Low	Lowest	Low
Energy Consumption	Medium	High	High	Highest	Medium	High	Low
Safety Risks	Small fragments and cuts	Small fragments, abrasive mud and cuts	Hazardous vapours, aerosol and burns	Hazardous vapours, dross and burns	Hazardous vapours, burns and gas explosions	Small fragments	Fragments and explosive waves
Environmental Impact	Medium	Medium	Low	Low	Medium	Medium	High
Ambient Applicability	All	All	Non Explosive	Non Explosive	Non Explosive	All	Non Explosive
Material Applicability	All Steels	All Steels and Composites	Non Reflective Steels	All Steels	All Steels, but mostly Carbon Steel	All Steels	All Steels
Maximum t_w	+300 mm	+300 mm	60 mm	50 mm	+300 mm	+300 mm	75 mm

2.1. AWJ technique for monopile foundation cutting

The performance of the AWJ technique for cutting the monopile foundations in the OWFs is highly dependent on the wall thickness. In this study, the cutting speeds of different techniques will be compared for different wall thicknesses of ISO EN 1.0577(S355J2) mild carbon steel tubular objects. Table 2 lists the cutting speeds of the AWJ technique for different wall thicknesses of ISO EN 1.0577(S355J2) mild carbon steel tubular objects which shows how the cutting speed of the AWJ is highly dependent on the thickness. The cutting speeds in Table 2 were calculated based on the calculation model provided by the KMT Waterjet Calculator [31].

Table 2. Cutting speeds of AWJ cutting technique depending on the wall thickness of S355J2 mild carbon steel tubular object (based on [31])

t_w (mm)	40	50	65	75	85	100	120	130	135	150
Cutting Speed (mm/min)	110.6	80.1	54.3	43.7	36.0	27.8	20.6	18.0	16.9	14.0

Due to their low thickness-to-length ratios, the monopile foundations can be considered thin-walled pipes with thicknesses between 40 mm and 150 mm. According to the definition stated by the American Society of Mechanical Engineering (ASME) [40], a thin-walled pipe is defined as a pipe if the ratio of wall thickness (t_w) to the outer diameter (D_o) is less than 1/6, i.e., $\frac{t_w}{D_o} < \frac{1}{6}$. This ratio for the monopile foundations is in the range between 1:10 and 1:53. Hence, the transient heat transfer analysis can be employed based on the assumption of 2D surface to

calculate the cooling time of the tubular monopile foundation wall with ISO EN 1.0577(S355J2) mild carbon steel material.

3. Cryogenic Cooling and Cutting System (CCCS)

The application of cryogenic cooling for the purpose of cutting carbon steel types using energy impact shattering is a novel idea and has not been widely addressed in the literature to date. This study's main aim is to theoretically investigate a novel embrittlement cutting technique, called CCCS, based on the cryogenic treatment approach. This section explains the overall idea, proof of concept, and the transient heat transfer model of the proposed CCCS technique.

In this study, the cutting process of S355J2 (ISO EN 1.0577) steel material will be investigated for the AWJ and CCCS techniques, which is one of the commonly used structural carbon steel types for large monopile foundation fabrication in OWFs [41], [42]. The cooling and cutting times required by the proposed CCCS technique for cutting the monopiles with different wall thicknesses will be compared to those yielded for the conventional non-thermal AWJ cutting technique. Figure 1 compares the overall conceptual designs of the proposed CCCS and conventional AWJ cutting techniques. The study will investigate the advantages of the novel cutting technique compared to the AWJ approach.

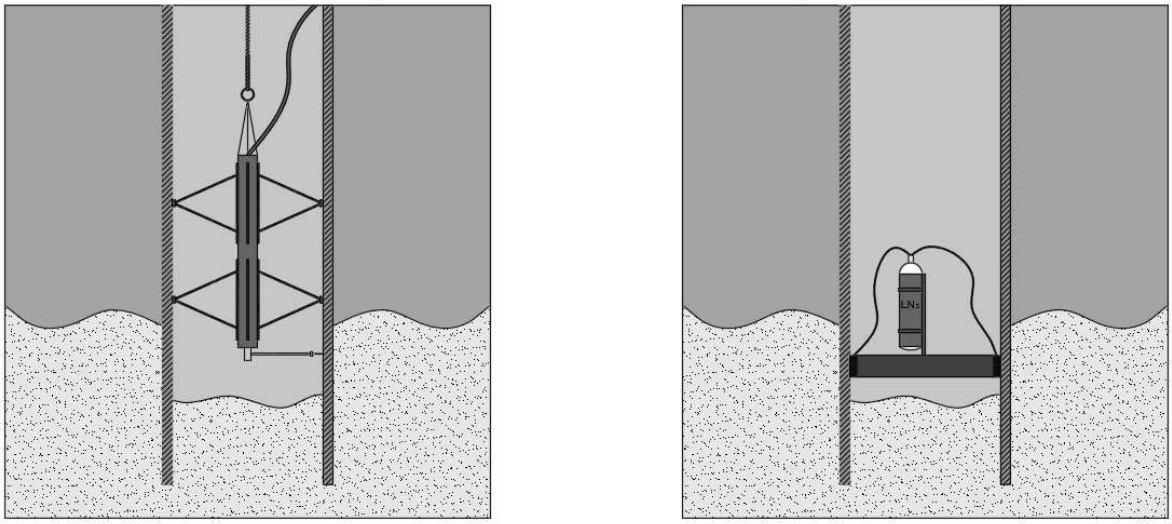

Figure 1. Comparison of cutting techniques: a) AWJ [43], b) new CCCS technique

The new Cryogenic Cooling and Cutting System (CCCS) consists of three main mechanical components as follows: i) the workpiece itself (i.e., the monopile), ii) the cooling system, and iii) the shattering mechanism. A detailed section view of the conceptual design of the CCCS with all main components is illustrated in Figure 2. The CCCS consists of two main parts, the cooling unit and the shattering mechanism. The former consists of the coolant housing halo, inlet and outlet for the cooling aid, as well as gaskets for a tight sealing against the inner surface of the monopile wall. The latter includes a clever to fracture the monopile wall, a shattering pin, a gasket around the cleaver for sealing the coolant from leaking out, a spring for rebounding the

shattering pin to its base point for refracturing, if needed, as well as the pneumatic pressure release for generating the required kinetic energy for the fracturing process.

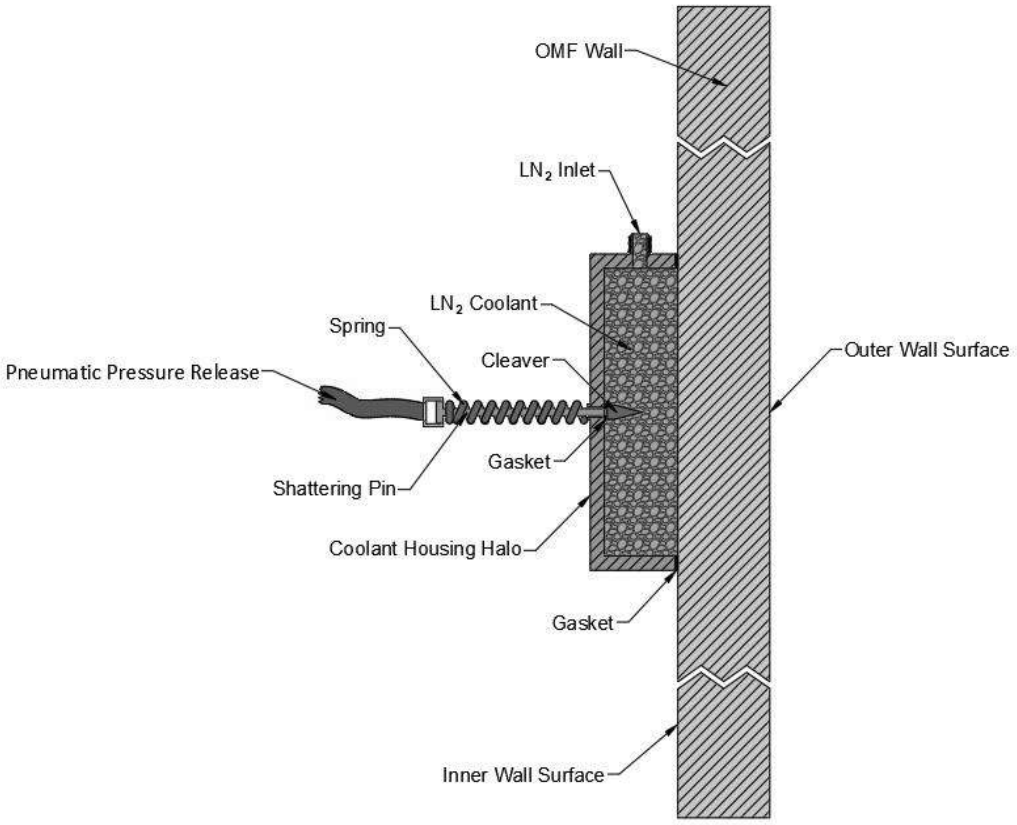

Figure 2. Conceptual design of the CCCS

3.1. Proof of concept

For the proof of concept of the new CCCS technique, the following questions are needed to be addressed to show how the proposed technique works:

- What coolant temperature is required to obtain a reasonable cooling time?
- What is the required impact energy needed for fracturing?
- To what extent do the ambient conditions affect the cooling time?
- What is the impact of the pipe length on the cooling time? Is CCCS applicable to long pipes?
- How can the cooling bandwidth affect the cooling time in the CCCS?
- Is it possible to cool down the fracturing area of a thick steel pipe to below transition temperature in a short timeframe?

- Is the CCCS fast enough to compete with conventional cutting methods, such as AWJ?
- What are the benefits of the new CCCS technique from economic and time viewpoints?

To answer the aforementioned questions, a set of information and data are needed to determine the theoretical foundation and simulate the new cutting concept, which can be obtained through a literature review. This study employs a two-dimensional transient heat transfer analysis based on the Finite Difference Method (FDM) to model the CCCS technique and obtain the cooling time and the kerf within an S355J2 mild carbon steel object.

The cutting time required by the CCCS technique depends on a set of parameters, such as the material properties, liquefied coolant type, the elemental composition of the material, the wall thickness t_w and outer diameter D_o of the monopile, the environmental condition, wind speed, and atmospheric conditions. Table 3 presents the elemental composition of S355J2 mild carbon steel assumed in this study. The S355J2 mild carbon steel has a material density (ρ) of 7850kg/m^3 [44], [45], thermal conductivity (k) of 50 W/mK [46], specific heat capacity (C_ρ) of 470 J/kgK [46], and a Charpy V-Notch (CVN) impact test strength of 27 J/cm^2 at -20 °C [13], [44]. The environmental condition is assumed as equivalent to the normal atmospheric conditions. The environmental heat transfer coefficient h depends on the wind speed v, which can be calculated by the following empirical equation [47]:

$$h = 12.12 - 1.16v + 11.6v^{1/2} \quad (1)$$

where the wind speed is between 1 m/s and 25 m/s, i.e., $1 \leq v \leq 25$. As the CCCS is an internal cutting technique, the minimum environmental heat transfer coefficient of 22.5 W/m^{2}K calculated by equation (1) based on the lower wind speed bound with the ambient temperature of 20°C is considered in this study.

Table 3. Elemental composition of ISO EN 1.0577 (S355J2) mild carbon steel [42], [44], [48]

Iron (Fe)	Carbon (C)	Manganese (Mn)	Phosphorus (P)	Sulphur (S)	Silicon (Si)	Copper (Cu)
97.03 Min	0.22 Max	1.60 Max	0.025 Max	0.025 Max	0.55 Max	0.55 Max

As was mentioned earlier, the monopile foundation is cut under the seabed, where the mud compound of the bedrock acts as an insulator against the saline water. As the heat transfer coefficient of the ocean's saline water will not affect the cooling process of the CCCS, this study neglects its impact on the transient heat transfer model. Rather, the heat transfer coefficient in equation (1) for stagnant air is used.

In the CCCS, a coolant needs to be applied to the surface of the carbon steel object before the cutting process takes place. This study assumes that the LN_2 is chosen for this purpose due to its appropriate cryogenic properties and prevalence in the industry. The application of LN_2 as a cooling aid reduces the energy absorption capability of steel objects and makes them ready for

the cutting process with minimum energy. To this end, it is assumed that the LN_2 is applied to the material surface with a coolant bandwidth size of between 50 mm and 500 mm. It is also assumed that the operational environmental pressure is 1 ATM or 1013 MPa, which implies that the working temperature of the LN_2 is equal to 77K (-196 °C) [49], [50], as can be seen from the thermodynamic phase diagram of nitrogen in Figure 3. In Figure 3, the Antoine vapour-pressure equation [51], [52] was used to calculate the LN_2 temperature based on its pressure. According to Refs. [53], [54], the LN_2 behaviour would be within the film boiling area if the difference between the LN_2 and ambient temperatures, represented by ΔT, be greater than about 120K (120°C). Considering the DBTT of the mild carbon steel at -45°C, the temperature difference between the LN_2 and the carbon steel will never reach below 140K during the cooling processes of the CCCS. Since the parameter ΔT for the CCCS condition will always be greater than the mentioned limit, the LN_2 will never reach its film boiling region. This means the LN_2 will provide efficient cooling properties for the cutting conditions in this study. In this study, the heat transfer coefficient of the LN_2 will be assumed to be about 128 W/m^2K considering the film boiling effect of ΔT taking place in the LN_2 when it comes into contact with warmer surface mild carbon steel objects, as evidenced by Refs. [54]–[57].

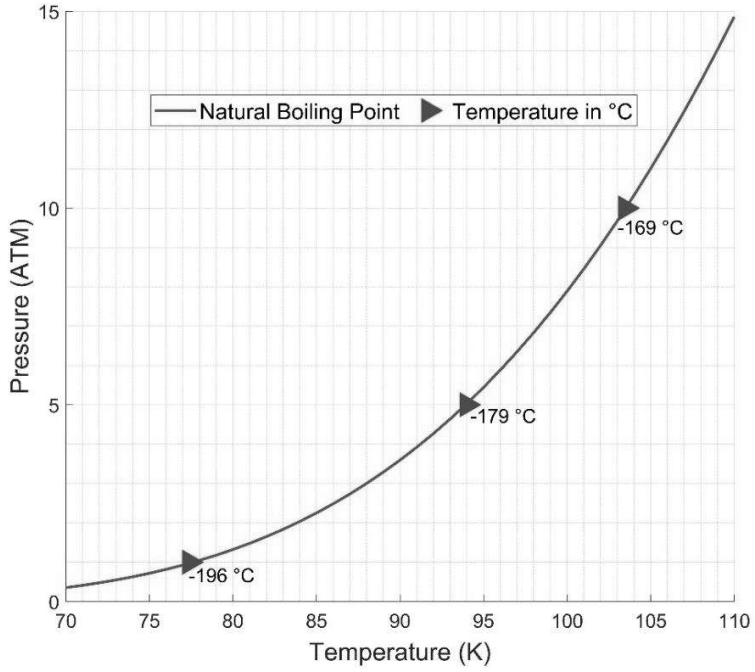

Figure 3. Thermodynamic phase diagram of LN_2 [50]

Figure 4 illustrates the transitional phase diagram of carbon steel types and their energy absorption capabilities adopted from [29], [58]. According to the International Organisation for Standardisation (IOS) [45] and ASME [40], the DBTT temperature of the S355J2 mild carbon steel is about -45 °C which results in 15 J/cm^2 of absorbed energy, as shown in Figure 4. In the CCCS, it is assumed that the temperature of the monopile steel wall will be reduced to -45 °C before the cutting process takes place. Then, the cutting process will be instant by applying a

pneumatic spring-loaded cleaver mechanism, which will add a maximum of 5 seconds to the cutting time of the CCCS according to the knowledge of the authors in fracture simulation tests of the cutting process.

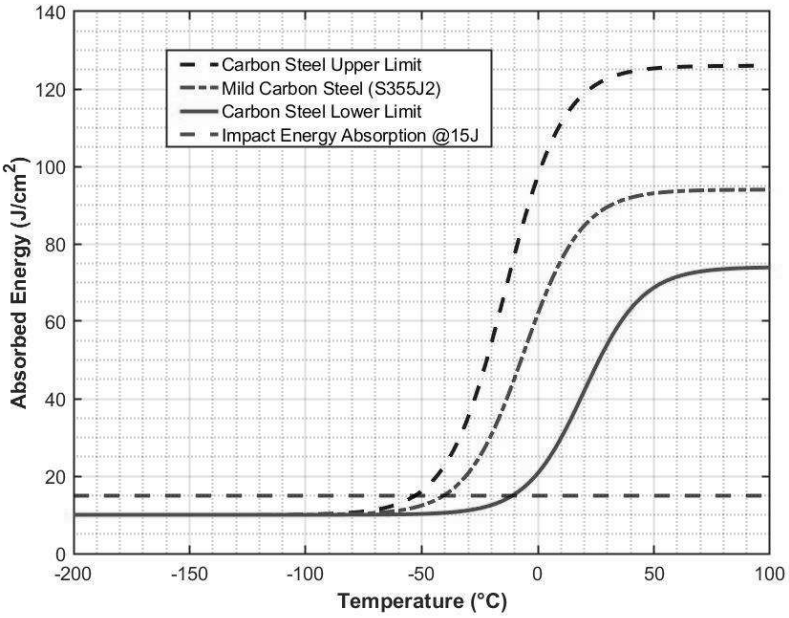

Figure 4. The transitional phase diagram of carbon steel types and the DBTT point for the S355J2 steel (J/cm^2) [29], [58]

To simulate the cutting process using the new CCCS technique, a transient heat transfer program was implemented in MATLAB, and the required cooling time to reach -45°C at the bottom surface of the S355J2 mild carbon steel object with the different wall thicknesses is calculated. Then, the overall durations required by the CCCS for cooling and cutting the S355J2 mild carbon steel object will be compared to the cutting times required by the conventional AWJ technique. The comparisons will be provided to show how the new CCCS technique can provide higher kerf quality and reduce the cutting time and environmental impact.

The two important parameters affecting the performance of cutters in OWF monopile foundations are the wall thickness and diameter. The thickness and diameter of the monopile foundation are usually designed against fatigue and buckling loads [59]. Literature review shows that the diameter of the monopile foundation can vary in a range from 2.5 m to 10.0 m, while its thickness can be between 40 mm and 150 mm [13], [60]–[66]. Therefore, this study focuses on the monopile foundations with the wall thicknesses of $t_{\mathrm{w}} \in [40\ \mathrm{m}, 150\ \mathrm{m}]$ and diameters of $D_{\mathrm{o}} \in [2.5\ \mathrm{mm}, 10\ \mathrm{mm}]$.

The CCCS will apply the cryogenic liquid to impact the atomic crystal structure in the cutting area of the monopile steel wall. The main aim of the new CCCS cutting concept is to cool down the monopile steel wall temperature in order to reach the DBTT temperature at which the impact

energy absorption capability of the steel is about 15 J/cm2, as shown in Figure 4e impact energy absorption of the S355J2 steel at an ambient temperature is about 27 J/cm^2, according to the impact v-notch test [67] and the carbon steel type specification of S355J2 [40]. Hence, the CCCS will cool down the steel to reduce the impact energy absorption from 27 J/cm^2 to 15 J/cm^2, which will make the monopile steel wall significantly brittle and easy to fracture. In order to prove the CCCS concept, Figure 5 presents the impact of the monopile length on the cooling time required to achieve the DBTT temperature of the S355J2 mild carbon steel monopile with a thickness of 50 mm and cooling bandwidth of 200 mm. From Figure 5, it can be seen that the cooling times are constant for the monopiles with longer lengths. According to Figure 5, the required cooling time in the CCCS is less than 897 seconds or 15 minutes, which is much less than the overall cutting time required by the AWJ technique and proves the advantage of the new embrittlement cutting concept.

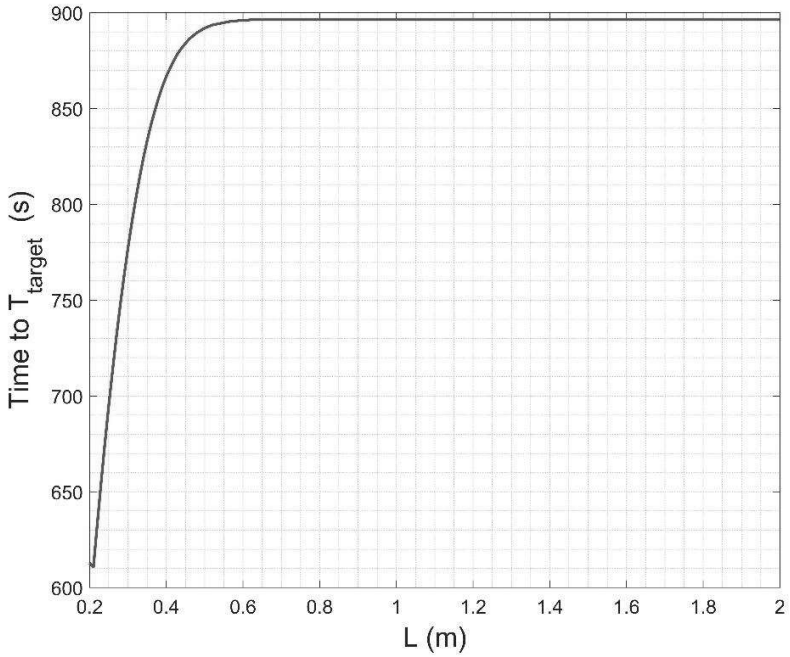

Figure 5. The impact of the monopile length on the cooling time of the S355J2 mild carbon steel monopile with a thickness of 50 mm and cooling bandwidth of 200 mm

3.2. Finite Difference Method (FDM) for the cooling process

To show the efficiency of the CCCS concept in terms of the cost and time, the cooling times need to be calculated for monopile foundations with different geometrical specifications. The cooling times are obtained through the transient heat transfer analysis based on the FDM. As the monopile foundations in OWFs are thin-walled tubular hollow structural systems, they can be modelled as a 2D linear surface model in the transient heat transfer calculations using FDM [68]. In comparison to a full 3D model, the application of 2D surface model of the tubular monopile foundations will make it easier to solve, handle, and calculate the cooling time required to reach the DBTT point at the cutting area. A program was developed in MATLAB to perform the 2D FDM analysis of the monopile structure and calculate the cooling times. To perform the transient

heat transfer analysis, a 2D nodal grid layout is considered for the cutting surface on the S355J2 mild carbon steel wall. Figure 6 illustrates a general monopile foundation, the cooling band, and the FDM area assumed by this study in the transient heat transfer analysis.

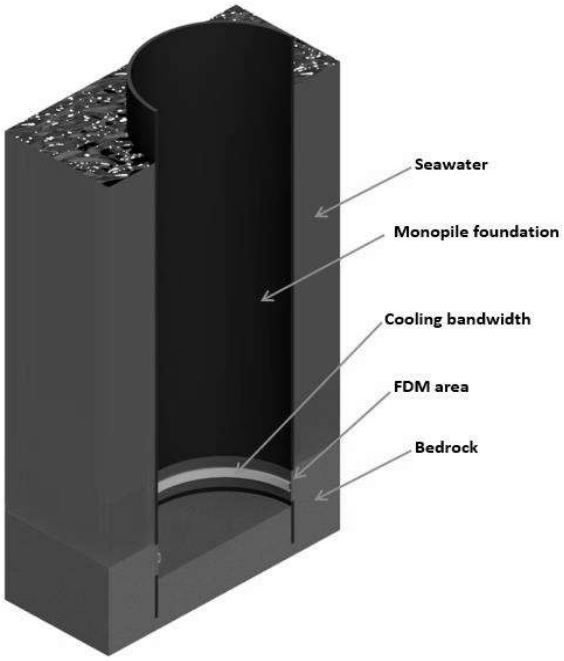

Figure 6. 3D model of the monopile foundation with the internal cryogenic cooling bandwidth (in yellow) and the FDM area (in red)

4. Numerical results

This section investigates the performance and potential applicability of the proposed CCCS technique in cutting the monopile foundation of WTs from different perspectives. The first subsection focuses on the impact of ambient temperature on the cooling times of CCCS. The cooling bandwidth and thickness are important parameters which could potentially affect the cooling time. The second subsection investigates the impacts of cooling bandwidth size and wall thicknesses on the cooling times of CCCS. The third subsection discusses the impact of monopile length on the required cooling times in the CCCs. Then, the fourth subsection provides an overall performance comparison between the proposed CCCS and AWJ cutting techniques in terms of cutting speeds and times. In the last subsection, the potential benefits of the CCCS technique in reducing the durations and costs of offshore operations in real-world OWF decommissioning projects are discussed.

In order to investigate the efficiency of the proposed CCCS technique, the results in this section are based on the FDM-based transient heat transfer analysis for the monopile foundations of the eight different offshore WTs listed in Table 4. The transient heat transfer analysis is performed

by assuming the LN_2 as the cooling aid, and the model's cooling band with 300 mm in length is considered to calculate the cooling time. As the cooling and cutting processes in the CCCS take place inside the monopile structure, the internal wind speed of the air is taken as equal to zero in the heat transfer analysis model. Considering the cutting conditions below the mudline, the ambient temperature of bedrock is assumed to be 20 °C, and the ambient bedrock's constant heat transfer coefficient is considered equal to 22.5 W/m^{2}K [47].

Table 4. The outer diameter (D_o) and wall thickness (t_w) of the monopile foundations investigated in this study

WT size (MWh):	5.0	2.0	2.0	3.0	3.6	10.0	5.5	6.0
D_o (mm):	2500	3000	3400	3400	4000	7500	8000	10000
t_w (mm):	130	40	50	120	65	85	135	150

4.1. Impact of ambient temperature on cooling times

To investigate how the ambient temperature can affect the cooling time of the monopile steel wall section, the required cooling times are calculated for different ambient temperatures, as shown in Figure 7. From Figure 7, the cooling time is significantly sensitive to the ambient temperature around the monopile foundation. It is observable that the cooling time for the ambient temperature of 0 °C is about 21 minutes and 21 seconds, while it is calculated around 33 minutes and 15 seconds for the ambient temperature equal to 20 °C. This highlights the necessity of an appropriate assumption on the ambient temperature around the steel monopile foundation. As was discussed earlier, the monopile foundation is usually cut 1 m below the seabed, which means that the heat transfer coefficient of the ocean saline water will not affect the cooling process of the proposed cutting technique. Hence, this study assumes the ambient temperature of 20 °C with a constant heat transfer coefficient equal to 22.5 W/m^{2}K [47] for the proposed novel CCCS technique.

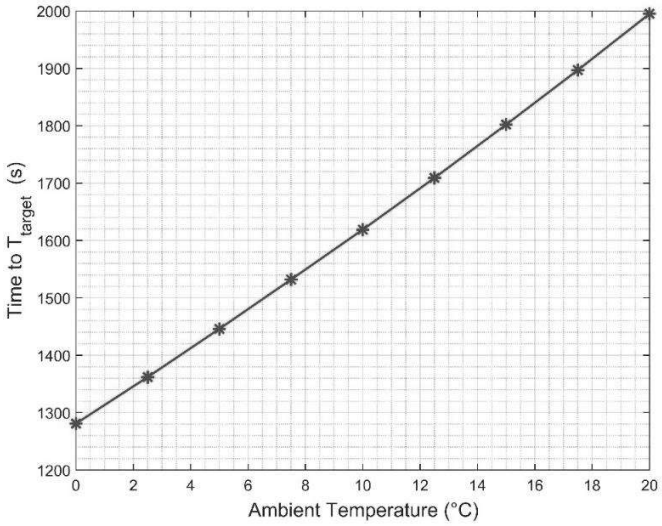

Figure 7. The cooling times required to reach -45 °C in the cutting area of the S355J2 carbon steel with a thickness of 100 mm

4.2. Impact of cooling bandwidth and thickness on the cooling time

The cooling bandwidth and the wall thickness of the monopile foundation can affect the cooling time required by the proposed CCCS technique. In order to show the extent of their impact, the cooling times required by the CCCS technique to reduce the temperature of the fracturing area on the monopile wall by -45°C are calculated for different bandwidth and wall thickness values, as shown in Figure 8. From Figure 8, it can be observed that increasing the cooling bandwidth on the monopile wall results in a faster cooling process and lower cooling times for different thicknesses. It also can be seen that the impact of cooling bandwidth on the cooling time becomes negligible for the higher bandwidth values, which shows excessively wider cooling bandwidths will increase the coolant costs without significant reductions in the cutting times. Hence, the optimal cooling bandwidth should be calculated for each monopile foundation with a specific thickness value. Based on the diagrams in Figure 8, the appropriate cooling bandwidths can be recommended for three categories of monopile foundations depending on their thicknesses, as follows:

$$b = \begin{cases} 250\ \text{mm} & \text{if } 40\ \text{mm} \le t_w \le 75\ \text{mm} \\ 300\ \text{mm} & \text{if } 80\ \text{mm} \le t_w \le 115\ \text{mm} \\ 400\ \text{mm} & \text{if } 120\ \text{mm} \le t_w \le 150\ \text{mm} \end{cases} \quad (2)$$

where b represents the cooling bandwidth and t_w is the monopile wall thickness. Although it is not possible to recommend an optimal cooling bandwidth value for all monopile types, it seems to be a good idea to consider an average cooling bandwidth of 300 mm for all monopile types.

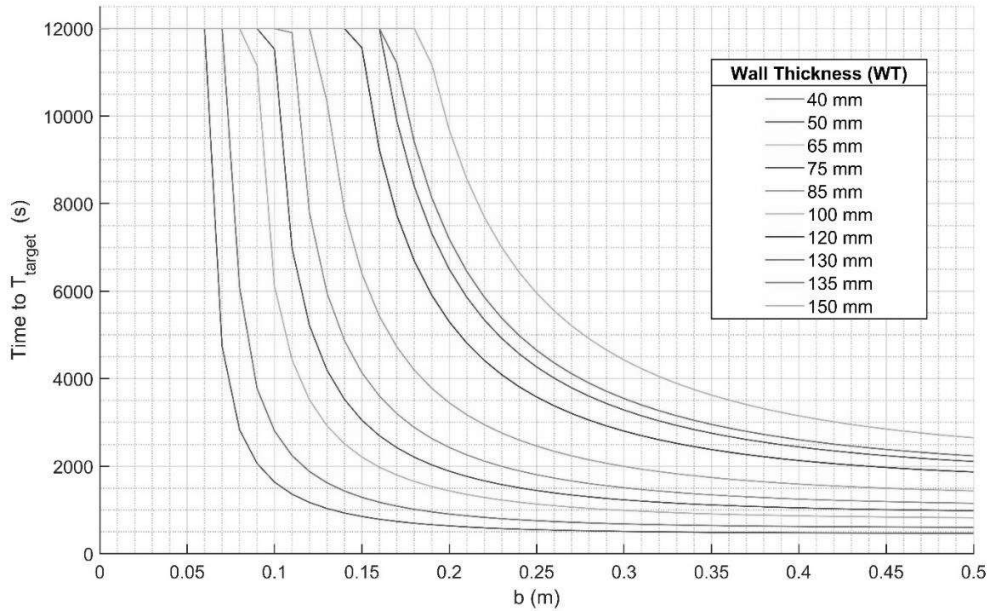

Figure 8. The cooling times required by CCCS to reduce the temperature of the fracturing area on the monopile wall to -45°C for different bandwidth and wall thickness values

4.3. Impact of monopile length on the cooling time

In this subsection, the impact of monopile length on the required cooling time of the proposed CCCS technique is investigated. Figure 9 shows the cooling time required in the CCCS cutting technique for different monopiles with different wall thicknesses and cooling bandwidth values. As can be observed from Figure 9, the cooling time does not change and remains constant for the monopiles with a greater than 1 m in length. This reveals the fact that the cooling time in the CCCS technique is not sensitive to the length of the monopiles with more than 1 m in length. Since the common monopile foundations in the OWFs are greater than 15 m in length due to stability requirements [65], it can be concluded that the impact of the monopile lengths on the cooling time of the CCCS technique is negligible.

4.4. Cutting time comparison

In order to show the effectiveness of the proposed embrittlement-based cutting technique, this subsection provides a performance comparison between the proposed CCCS and conventional AWJ cutting techniques. Table 5 presents the performance comparison between the CCCS and conventional AWJ techniques in cutting monopile foundations of different WTs, which shows the cutting speeds and times, assumed bandwidths, and time savings. Table 5 shows that the cutting speeds of the CCCS technique are from 7.7 up to 46.8 times faster than the AWJ technique depending on the monopile diameters and wall thicknesses, which result in 87.1% up to 97.9% reductions in cutting times.

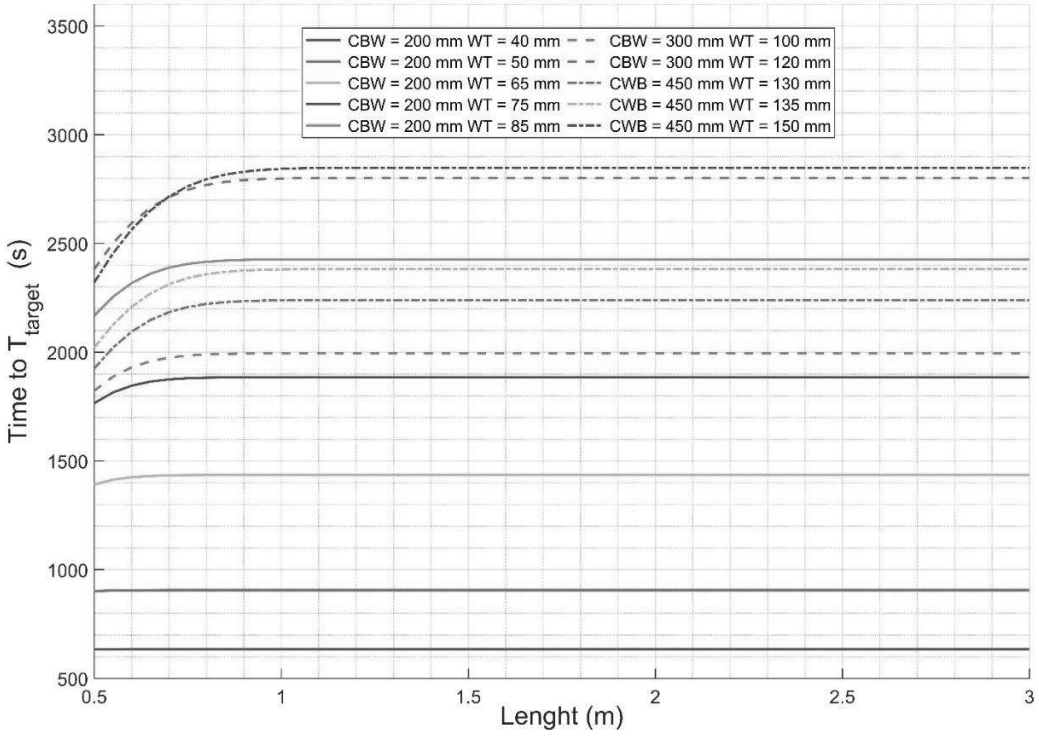

Figure 9. The cooling times required by CCCS to reduce the temperature of the fracturing area on the monopile wall by -45°C for different cooling bandwidth, wall thickness, and length values

4.5. Potential cost savings in OWF decommissioning projects

The OWF decommissioning operations are usually performed by a set of vessels/equipment with significant leasing costs. As was mentioned earlier, foundation removal is one of the expensive operations in the OWF decommissioning projects. The monopile foundations need to be cut at an appropriate depth under the seabed. The literature survey shows that most of the OWF decommissioning projects employ a JUV to support the cutting process and lift the foundation. The approach also requires a desired number of BVs and TBs for the transportation of dismantled foundations to shore. The faster cutting times can result in significant reductions in vessel costs. The intention of this subsection is to show to what extent the proposed CCCS cutting technique can reduce the foundation removal costs in OWF decommissioning projects.

Table 5. Performance comparison between the proposed CCCS and conventional AWJ cutting techniques

	1	2	3	4	5	6	7	8
WT size (MW)	5.0	2.0	2.0	3.0	3.6	10.0	5.5	6.0
D_o (mm)	2500	3000	3400	3400	4000	7500	8000	10000
Circumference length (mm)	7854	9425	10681	10681	12566	23562	25133	31416
t_w (mm)	130	40	50	120	65	85	135	150
AWJ cutting speed (mm/min) [31]	18.0	110.6	80.1	20.6	54.3	36.0	16.9	14.0
AWJ cutting time (min) [31]	436	85	133	518	231	655	1487	2244
Cooling bandwidth (mm)	450	200	200	450	200	200	450	200
CCCS cutting time (min)	37.5	11.0	15.5	33.0	24.0	41.0	40.0	48.0
Time savings (%)	91.4%	87.1%	88.1%	93.6%	89.6%	93.7%	97.3%	97.9%

In order to show the cost-benefit of the CCCS over the conventional AWJ technique, let us consider Cape Wind OWF decommissioning projects in the US. This OWF consisted of 101 WTs with a 3.6 MW capacity per unit. The diameter of monopile foundations in this OWF is equal to 16.4 ft, and the wall thickness is equal to 95 mm. The available data from the Cape Wind decommissioning programme shows that the foundation removal operation using the AWJ cutting technique was estimated to take about 151.5 days, resulting in 1.5 days per WT unit [69], [70]. The monopile foundation removal operation usually takes place in three stages, including preparation, cutting, and lifting stages. Since a prototype for the proposed embrittlement-cutting method has yet to be developed, the intention of this subsection is to show the cost-benefit of the CCCS only in terms of cutting duration.

According to Ref. [31], the cutting speed internal AWJ technique is about 30.2 mm/min, which will result in a cutting time of 8 hours and 40 mins for a monopile foundation with a thickness of 95 mm. This means the preparation and lifting stages of each foundation in the Cape Wind OWF take place in about 27 hours and 20 mins. When it comes to the CCCS technique, requires significantly less cutting time compared to the AWJ technique. The CCCS requires only about 24 mins to cut the same monopile foundation, which offers more than 95% saving in cutting

time. By considering the cutting times required by the CCCS, the total removal duration of 101 monopile foundations in the Cape Wind OWF will reduce from 151.5 days to about 117 days, which shows a reduction of 28% in overall operational time. Figure 10 shows the resulting foundation removal durations using the new CCCS and conventional AWJ techniques for different numbers of monopiles. As can be seen from this figure, the advantage of applying the new CCCS is more obvious for the OWFs with a larger number of monopiles.

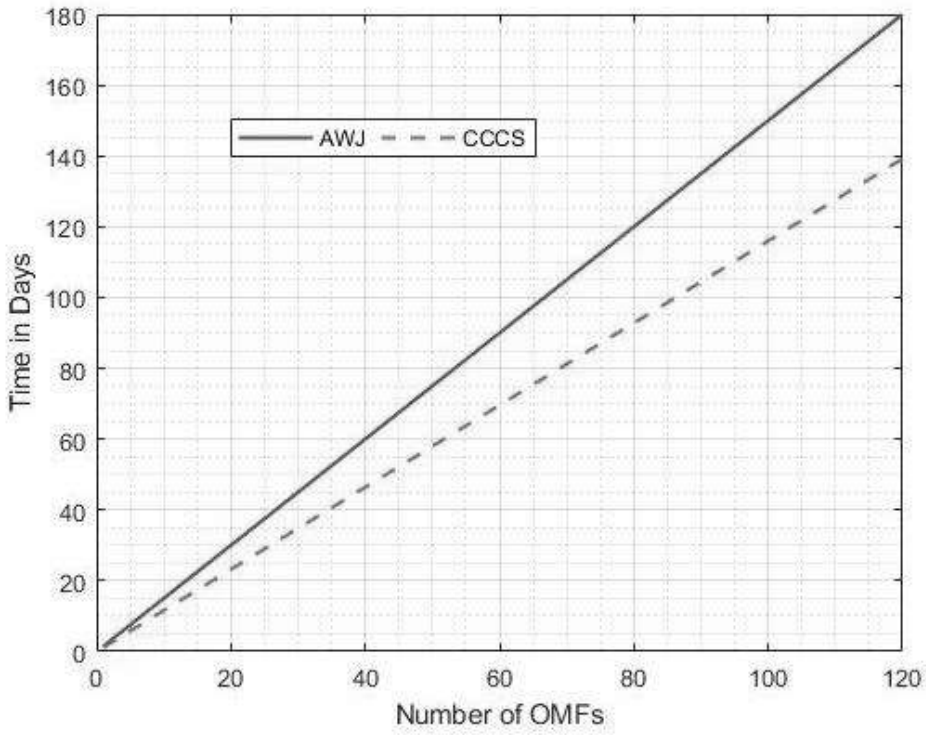

Figure 10. The resulting foundation removal durations using the AWJ and CCCS techniques for different numbers of monopiles

According to the previous data available from OWF decommissioning, the leasing rates of the vessels employed for foundation removal operation vary and depend on various parameters, such as duration of the contract, inflation rate, and market situation [71]. However, the minimum day rates for the JUV, BV, and TB can be considered about £100 k, £12.9 k, and £8.6 k, respectively [71], [72]. By considering these assumptions, Table 6 compares the vessel costs obtained for the foundation removal operation using different cutting techniques in the Cape Wind OWF with 101 monopiles. From Table 6, the overall vessel cost obtained using the CCCS technique is about £14.31 m, while it is about £18.40 m for the conventional AWJ technique. This shows more than £4 m reduction in overall foundation removal costs, about 23% saving in the vessel leasing costs. The results highlight the fact the development of innovative foundation-cutting technologies plays a key role in reducing the cost of wind energy production.

Table 6. The vessel costs for the foundation removal operation in the Cape Wind OWF with 101 monopiles using CCCS and AWJ cutting techniques

		AWJ				CCCS			
Vessel	Leasing rate (£/day)	Duration per monopile	Overall duration	Cost per monopile (£)	Overall cost (£)	Duration per monopile	Overall duration	Cost per monopile (£)	Overall cost (£)
JUV	100 k	1.50	151.50	150 k	15.15 m	1.16	117	116 k	11.7 m
BV	12.9 k	1.50	151.50	19.35 k	1.95 m	1.16	117	15 k	1.51 m
TB	8.6 k	1.50	151.50	12.9 k	1.30 m	1.16	117	10 k	1.10 m
				Total:	**18.40 m**			**Total:**	**14.31 m**

5. Concluding remarks

The study presented a feasibility study on a novel CCCS technique for the cutting operation of monopile foundations in the OWFs. The main idea of the study is based on the cryogenic treatment, which is applied to the cutting surface of the steel object to reduce its impact energy absorption capability and achieve faster cutting speeds in comparison to conventional cutting techniques. The overall idea and proof of concept were presented and the cutting process using the CCCS was simulated using an FDM-based transient heat transfer model. The performance of the CCCS depends on different parameters, such as ambient temperature, cooling bandwidth, and monopile length. The numerical results obtained from the heat transfer analysis revealed that the selection of appropriate cooling bandwidth on the monopile surface is crucial. Based on the results, it was shown that higher cooling bandwidths result in a faster cooling process and lower cooling times for different wall thicknesses. Meanwhile, the impact of cooling bandwidth on the cooling time becomes negligible for the higher bandwidth values, which shows excessively wider cooling bandwidths will increase the coolant costs without significant reductions in the cutting times. The performance comparisons between the CCCS and the traditional AWJ cutting technique suggested that the cutting speeds of the CCCS technique are from 7.7 up to 46.8 times faster than the AWJ technique depending on the monopile diameters and wall thicknesses, which result in 87.1% up to 97.9% reductions in cutting times. The potential economic benefits of the new CCCS cutting technique over the traditional AWJ technique were also investigated on a real-world OWF decommissioning project. The results of the OWF case study, which consisted of 101 foundations, showed that the CCCS could reduce the total foundation removal operation time by 28%, which results in 23% saving in vessel leasing costs. Future studies can be focused on the experimental investigation of CCCS for the offshore cutting operations of monopile foundations.

Acknowledge

This paper is partly based on the work undertaken for the project 'Eco-innovative concepts for the end of offshore wind energy farms lifecycle' (DecomTools). The project has received funding from the European Commission under the Interreg VB North Sea Region Programme. Project No.: 20180305091606.

References:

[1] International Renewable Energy Agency, "Future of wind," Oct. 2019. https://irena.org/publications/2019/Oct/Future-of-wind (accessed Jul. 20, 2022).

[2] The Crown State, "Offshore wind operational report 2020," 2020. Accessed: Jun. 15, 2022. [Online]. Available: https://www.thecrownestate.co.uk/media/3792/offshore-wind-operational-report-1.pdf

[3] Rystad Energy, "UK's renewable energy capacity set to double by 2026, when offshore wind will overtake onshore," 2020. https://www.rystadenergy.com/newsevents/news/press-releases/uks-renewable-energy-capacity-set-to-double-by-2026-when-offshore-wind-will-overtake-onshore/ (accessed Jun. 15, 2022).

[4] M. Vieira, B. Snyder, E. Henriques, and L. Reis, "European offshore wind capital cost trends up to 2020," *Energy Policy*, vol. 129, pp. 1364–1371, Jun. 2019, doi: 10.1016/j.enpol.2019.03.036.

[5] Wind Europe, "Our energy, our future: How offshore wind will help Europe go carbon-neutra," Nov. 2019. https://windeurope.org/about-wind/reports/our-energy-our-future/ (accessed Jul. 20, 2022).

[6] R. Lacal-Arántegui, J. M. Yusta, and J. A. Domínguez-Navarro, "Offshore wind installation: Analysing the evidence behind improvements in installation time," *Renewable and Sustainable Energy Reviews*, vol. 92, pp. 133–145, Sep. 2018, doi: 10.1016/j.rser.2018.04.044.

[7] "DecomTools, Interreg VB North Sea Region Programme." https://northsearegion.eu/decomtools (accessed Jun. 15, 2022).

[8] Wind Power Monthly, "Dong announces Vindeby decommissioning," 2016. https://www.windpowermonthly.com/article/1382887/dong-announces-vindeby-decommissioning (accessed Jun. 15, 2022).

[9] Offshore Wind, "Vattenfall Wraps Up First Ever Offshore Wind Farm Decommissioning," 2016. https://www.offshorewind.biz/2016/01/25/vattenfall-wraps-up-first-ever-offshore-wind-farm-decommissioning/ (accessed Jun. 15, 2022).

[10] C. Mackie and A. P. M. Velenturf, "Trouble on the horizon: Securing the decommissioning of offshore renewable energy installations in UK waters," *Energy Policy*, vol. 157, p. 112479, Oct. 2021, doi: 10.1016/j.enpol.2021.112479.

[11] W. Njomo-Wandji, A. Natarajan, and N. Dimitrov, "Influence of model parameters on the design of large diameter monopiles for multi-megawatt offshore wind turbines at 50-m water depths," *Wind Energy*, vol. 22, no. 6, pp. 794–812, Jun. 2019, doi: 10.1002/we.2322.

[12] G. Cao, X. Ding, Z. Yin, H. Zhou, and P. Zhou, "A new soil reaction model for large-diameter monopiles in clay," *Comput Geotech*, vol. 137, p. 104311, Sep. 2021, doi: 10.1016/j.compgeo.2021.104311.

[13] B. K. Gupta and D. Basu, "Offshore wind turbine monopile foundations: Design perspectives," *Ocean Engineering*, vol. 213, p. 107514, Oct. 2020, doi: 10.1016/j.oceaneng.2020.107514.

[14] The Crown Estate & Offshore Renewable Energy Catapult, "Guide to an offshore wind farm," 2019. https://www.thecrownestate.co.uk/media/2860/guide-to-offshore-wind-farm-2019.pdf (accessed Jun. 08, 2022).

[15] M. S. Nazir, N. Ali, M. Bilal, and H. M. N. Iqbal, "Potential environmental impacts of wind energy development: A global perspective," *Curr Opin Environ Sci Health*, vol. 13, pp. 85–90, Feb. 2020, doi: 10.1016/j.coesh.2020.01.002.

[16] P. Jankovic, M. Madic, D. Petkovic, and M. Radovanovic, "Analysis and modeling of the effects of process parameters on specific cutting energy in abrasive water jet cutting," *Thermal Science*, vol. 22, no. Suppl. 5, pp. 1459–1470, 2018, doi: 10.2298/TSCI18S5459J.

[17] G. Guglielmi, B. Mitchell, C. Song, B. L. Kinsey, and W. Mo, "Life Cycle Environmental and Economic Comparison of Water Droplet Machining and Traditional Abrasive Waterjet Cutting," *Sustainability*, vol. 13, no. 21, p. 12275, Nov. 2021, doi: 10.3390/su132112275.

[18] K. Gu, J. Wang, and Y. Zhou, "Effect of cryogenic treatment on wear resistance of Ti–6Al–4V alloy for biomedical applications," *J Mech Behav Biomed Mater*, vol. 30, pp. 131–139, Feb. 2014, doi: 10.1016/j.jmbbm.2013.11.003.

[19] S. Akincioğlu, H. Gökkaya, and İ. Uygur, "A review of cryogenic treatment on cutting tools," *The International Journal of Advanced Manufacturing Technology*, vol. 78, no. 9–12, pp. 1609–1627, Jun. 2015, doi: 10.1007/s00170-014-6755-x.

[20] National Institute of Standards and Technology, "Cryogenic Technology Resources - About Cryogenics." https://trc.nist.gov/cryogenics/aboutCryogenics.html (accessed Oct. 24, 2022).

[21] Y. Li, Y. Chen, and X. Zhou, "Effects of Cryogenic Treatment and Tempering on Mechanical Properties and Microstructure of 0.25C-0.80Si-1.6Mn Steel," *Advances in Materials Science and Engineering*, vol. 2020, pp. 1–8, Oct. 2020, doi: 10.1155/2020/1501474.

[22] H. Zhang, X. Yan, Q. Hou, and Z. Chen, "Effect of Cyclic Cryogenic Treatment on Wear Resistance, Impact Toughness, and Microstructure of 42CrMo Steel and Its Optimisation," *Advances in Materials Science and Engineering*, vol. 2021, pp. 1–13, Jan. 2021, doi: 10.1155/2021/8870282.

[23] T. Sonar, S. Lomte, and C. Gogte, “Cryogenic Treatment of Metal – A Review,” *Mater Today Proc*, vol. 5, no. 11, pp. 25219–25228, 2018, doi: 10.1016/j.matpr.2018.10.324.

[24] D. Senthilkumar, I. Rajendran, and M. Pellizzari, "Effect of cryogenic treatment on the hardness and tensile behaviour of AISI 4140 steel," *International Journal of Microstructure and Materials Properties*, vol. 6, no. 5, p. 366, 2011, doi: 10.1504/IJMMP.2011.043573.

[25] P. Sivaiah and D. Chakradhar, "The Effectiveness of a Novel Cryogenic Cooling Approach on Turning Performance Characteristics During Machining of 17-4 PH Stainless Steel Material," *Silicon*, vol. 11, no. 1, pp. 25–38, Feb. 2019, doi: 10.1007/s12633-018-9875-3.

[26] N. Govindaraju, L. Shakeel Ahmed, and M. Pradeep Kumar, "Experimental Investigations on Cryogenic Cooling in the Drilling of AISI 1045 Steel," *Materials and Manufacturing Processes*, vol. 29, no. 11–12, pp. 1417–1421, Dec. 2014, doi: 10.1080/10426914.2014.930952.

[27] S. S. Muhamad, J. A. Ghani, C. H. C. Haron, and H. Yazid, "Cryogenic milling and formation of nanostructured machined surface of AISI 4340," *Nanotechnol Rev*, vol. 9, no. 1, pp. 1104–1117, Nov. 2020, doi: 10.1515/ntrev-2020-0086.

[28] S. Kumar, N. K. Khedkar, B. Jagtap, and T. P. Singh, "The Effects of Cryogenic Treatment on Cutting Tools," *IOP Conf Ser Mater Sci Eng*, vol. 225, p. 012104, Aug. 2017, doi: 10.1088/1757-899X/225/1/012104.

[29] C. M. Moura, J. J. Villela, E. G. Rabello, G. de P. Martins, and J. R. G. Carneiro, "Evaluation of the ductile-to-brittle transition temperature in steel low carbon," 2009.

[30] James Fisher and Sons plc, "Subsea shears." http://www.fisheroffshore.com/equipment/subsea-tooling/cutting/subsea-shears/ (accessed Jul. 20, 2022).

[31] KMT Shape Technology Group, "KMT Waterjet Calculator." https://www.kmtwaterjet.com/kmt-cut-calculator.aspx (accessed Jul. 21, 2022).

[32] H. Wegener, H. U. Freund, and St. Schumann, "Explosive cutting of thick-walled steel pipes in the reactor HDR," *Nuclear Engineering and Design*, vol. 118, no. 1, pp. 87–97, Mar. 1990, doi: 10.1016/0029-5493(90)90089-G.

[33] J. W. Brandon, B. Ramsey, J. W. Macfarlane, and D. Dearman, "Abrasive Water-Jet and Diamond Wire-Cutting Technologies Used in the Removal of Marine Structures," in *All Days*, May 2000. doi: 10.4043/12022-MS.

[34] E. Topham and D. McMillan, "Sustainable decommissioning of an offshore wind farm," *Renew Energy*, vol. 102, pp. 470–480, Mar. 2017, doi: 10.1016/j.renene.2016.10.066.

[35] J. S. Shin *et al.*, "Underwater cutting of 50 and 60 mm thick stainless steel plates using a 6-kW fiber laser for dismantling nuclear facilities," *Opt Laser Technol*, vol. 115, pp. 1–8, Jul. 2019, doi: 10.1016/j.optlastec.2019.02.005.

[36] M. st. Weglowski and T. Pfeifer, "Influence of a cutting technology on the quality of unalloyed steel surface," *Biuletyn Instytutu Spawalnictwa w Gliwicach*, vol. 58, no. 1, pp. 13–23, 2014.

[37] M. Brozek, "Steel cutting using abrasive water jet," May 2017. doi: 10.22616/ERDev2017.16.N014.

[38] S. Cicero *et al.*, "Fatigue behaviour of structural steels with oxy-fuel, plasma and laser cut straight edges. Definition of Eurocode 3 FAT classes," *Eng Struct*, vol. 111, pp. 152–161, Mar. 2016, doi: 10.1016/j.engstruct.2015.12.004.

[39] V. Peržel, S. Hloch, H. Tozan, M. Yagimli, and P. Hreha, "Comparative analysis of abrasive waterjet (AWJ) technology with selected unconventional manufacturing processes," *International Journal of Physical Sciences*, vol. 6, no. 24, pp. 5587–5593, 2011.

[40] "ASME B31.3-2020 - Process Pipe," New York, 2021.

[41] V. Igwemezie, A. Mehmanparast, and A. Kolios, "Materials selection for XL wind turbine support structures: A corrosion-fatigue perspective," *Marine Structures*, vol. 61, pp. 381–397, Sep. 2018, doi: 10.1016/j.marstruc.2018.06.008.

[42] V. Igwemezie and A. Mehmanparast, "Waveform and frequency effects on corrosion-fatigue crack growth behaviour in modern marine steels," *Int J Fatigue*, vol. 134, p. 105484, May 2020, doi: 10.1016/j.ijfatigue.2020.105484.

[43] N. Hinzmann, P. Stein, J. Gattermann, J. Bachmann, and G. Duff, "Measurements of hydro sound emissions during internal jet cutting during monopile decommissioning," in *COME-Conference on Maritime Energy 2017-Decommissioning of Offshore Geotechnical Structures, 28.-29. März 2017 in Hamburg, S. 139*, 2017, vol. 161.

[44] G. Arntsen, “Stål håndbogen,” Copenhagen.

[45] "International Organization for Standardization." ISO EN 10025-2:2019, Genève, 2019.

[46] "EN 1.0577 (S355J2) Non-Alloy Steel," *Makeitfrom.com*. https://www.makeitfrom.com/material-properties/EN-1.0577-S355J2-Non-Alloy-Steel (accessed Jul. 22, 2022).

[47] The Engineering Tool Box, "Convective Heat Transfer." https://www.engineeringtoolbox.com/convective-heat-transfer-d_430.html (accessed Jul. 22, 2022).

[48] M. K. Kulekci, "Processes and apparatus developments in industrial waterjet applications," *Int J Mach Tools Manuf*, vol. 42, no. 12, pp. 1297–1306, Sep. 2002, doi: 10.1016/S0890-6955(02)00069-X.

[49] D. J. Morris *et al.*, "Over 10 million seawater temperature records for the United Kingdom Continental Shelf between 1880 and 2014 from 17 Cefas (United Kingdom government) marine data systems," *Earth Syst Sci Data*, vol. 10, no. 1, pp. 27–51, Jan. 2018, doi: 10.5194/essd-10-27-2018.

[50] Dean J. and Lange N, "Lange's Handbook Of Chemistry," New York: McGraw-Hill, 2001, pp. 402–406.

[51] M. P. Edejer and G. Thodos, "Vapor pressures of liquid nitrogen between the triple and critical points," *J Chem Eng Data*, vol. 12, no. 2, pp. 206–209, Apr. 1967, doi: 10.1021/je60033a014.

[52] H. Kerkvliet and H. Polatidis, "Offshore wind farms' decommissioning: a semi quantitative Multi-Criteria Decision Aid framework," *Sustainable Energy Technologies and Assessments*, vol. 18, pp. 69–79, Dec. 2016, doi: 10.1016/j.seta.2016.09.008.

[53] J. Zhou, W. K. Chan, and J. Schwartz, "Quench Detection Criteria for YBa2Cu3O7-δ Coils Monitored via a Distributed Temperature Sensor for 77 K Cases," *IEEE Transactions on Applied Superconductivity*, vol. 28, no. 5, pp. 1–12, Aug. 2018, doi: 10.1109/TASC.2018.2815920.

[54] B. P. Breen, "Effect of Diameter of Horizontal Tubes of Film Boiling," University of Illinois at Urbana-Champaign, 1961.

[55] S. O. AWONORIN and J. LAMB, "Heat transfer coefficient for nitrogen droplets film-boiling on a food surface," *Int J Food Sci Technol*, vol. 23, no. 4, pp. 391–401, Jun. 2007, doi: 10.1111/j.1365-2621.1988.tb00594.x.

[56] Y. Liu, T. Olewski, L. Vechot, X. Gao, and S. Mannan, "Modelling of a cryogenic liquid pool boiling using CFD code," in *14th Annual Symposium, Mary Kay O'Connor Process Safety Center "Beyond Regulatory Compliance: Making Safety Second Nature*, 2011, pp. 512–524.

[57] T. Jin, J. Hong, H. Zheng, K. Tang, and Z. Gan, "Measurement of boiling heat transfer coefficient in liquid nitrogen bath by inverse heat conduction method," *Journal of Zhejiang University-SCIENCE A*, vol. 10, no. 5, pp. 691–696, May 2009, doi: 10.1631/jzus.A0820540.

[58] Dr. S. D. Kahar, "Duplex Stainless Steels-An overview," *Int J Eng Res Appl*, vol. 07, no. 04, pp. 27–36, Apr. 2017, doi: 10.9790/9622-0704042736.

[59] K. A. Schmoor and M. Achmus, "Optimum geometry of monopiles with respect to the geotechnical design," *J. Ocean Wind Energy*, vol. 2, no. 1, pp. 54–60, 2015.

[60] RGL, “Blyth - Removal of Wind Turbine Monopiles Project.” https://express.adobe.com/page/DYJscZF3F8417/ (accessed Jul. 25, 2022).

[61] Y.-S. Lee, B.-L. Choi, J. H. Lee, S. Y. Kim, and S. Han, “Reliability-based design optimisation of monopile transition piece for offshore wind turbine system,” *Renew Energy*, vol. 71, pp. 729–741, Nov. 2014, doi: 10.1016/j.renene.2014.06.017.

[62] S. Wang, T. J. Larsen, and H. Bredmose, “Ultimate load analysis of a 10 MW offshore monopile wind turbine incorporating fully nonlinear irregular wave kinematics,” *Marine Structures*, vol. 76, p. 102922, Mar. 2021, doi: 10.1016/j.marstruc.2020.102922.

[63] M. B. Zaaijer, “Foundation modelling to assess dynamic behaviour of offshore wind turbines,” *Applied Ocean Research*, vol. 28, no. 1, pp. 45–57, Feb. 2006, doi: 10.1016/j.apor.2006.03.004.

[64] Carbon Trust, “Carbon Trust Offshore Wind Accelerator announces winners of Subsea Inspection competition,” 2018. https://www.carbontrust.com/news-and-events/news/carbon-trust-offshore-wind-accelerator-announces-winners-of-subsea-inspection (accessed Jul. 25, 2022).

[65] S. Peder Hyldal Sørensen and L. Bo Ibsen, “Assessment of foundation design for offshore monopiles unprotected against scour,” *Ocean Engineering*, vol. 63, pp. 17–25, May 2013, doi: 10.1016/j.oceaneng.2013.01.016.

[66] L. Wang, Y. Lai, Y. Hong, and D. Mašín, “A unified lateral soil reaction model for monopiles in soft clay considering various length-to-diameter (L/D) ratios,” *Ocean Engineering*, vol. 212, p. 107492, Sep. 2020, doi: 10.1016/j.oceaneng.2020.107492.

[67] ASTM International, “ASTM E23-18: Standard Test Methods for Notched Bar Impact Testing of Metallic Materials.” https://www.astm.org/e0023-18.html (accessed Jul. 25, 2022).

[68] Y. A. Cengel, *Heat transfer: a practical approach*. 1997.

[69] PCCI, “Decommissioning cost estimations for the Cape Wind Energy project.” https://www.boem.gov/sites/default/files/renewable-energy-program/Studies/PCCI-Cape-Wind-Decommissioning-Final-Report.pdf (accessed Jul. 26, 2022).

[70] C. Milne, S. Jalili, and A. Maheri, “Decommissioning cost modelling for offshore wind farms: A bottom-up approach,” *Sustainable Energy Technologies and Assessments*, vol. 48, p. 101628, Dec. 2021, doi: 10.1016/j.seta.2021.101628.

[71] Jalili et al., “Cost modelling for offshore wind farm decommissioning,” 2022. Accessed: Dec. 01, 2022. [Online]. Available: https://northsearegion.eu/decomtools/news/cost-modelling-for-offshore-wind-farm-decommissioning/

[72] J. A. Quintana, “Alternative Installation Methods for Offshore Wind Substations,” *Department of Mechanical and Aerospace Engineering, University of Strathclyde*, 2016.